

Electronic Supplementary Information for

## **Dehydration impeding ionic conductance through two-dimensional angstrom-scale slits**

YanZi Yu, JingCun Fan, Jun Xia, YinBo Zhu, HengAn Wu and FengChao Wang\*

CAS Key Laboratory of Mechanical Behavior and Design of Materials, Department of Modern Mechanics, CAS Center for Excellence in Complex System Mechanics, University of Science and Technology of China, Hefei, Anhui 230027, China.

\*Email: [wangfc@ustc.edu.cn](mailto:wangfc@ustc.edu.cn)

**I. Table S1. Lennard-Jones parameters of molecular dynamics (MD) simulations.**

	$\sigma(\text{\AA})$	$\epsilon(\text{kcal/mol})$
O-O <sup>S1</sup>	3.166	0.1554
H-H <sup>S1</sup>	0	0
C-O <sup>S2</sup>	3.436	0.0850
C-H <sup>S2</sup>	2.69	0.0383
C-C <sup>S3</sup>	3.39	0.0692
Mg <sup>2+</sup> <sup>S4</sup>	2.546	0.0209
Ca <sup>2+</sup> <sup>S4</sup>	2.912	0.0973
Cl <sup>-</sup> <sup>S5</sup>	4.831	0.0128
K <sup>+</sup> <sup>S5</sup>	2.838	0.4297
Li <sup>+</sup> <sup>S5</sup>	1.409	0.3367
Na <sup>+</sup> <sup>S5</sup>	2.160	0.3526

**II. Discussion on the polarization of graphene.**

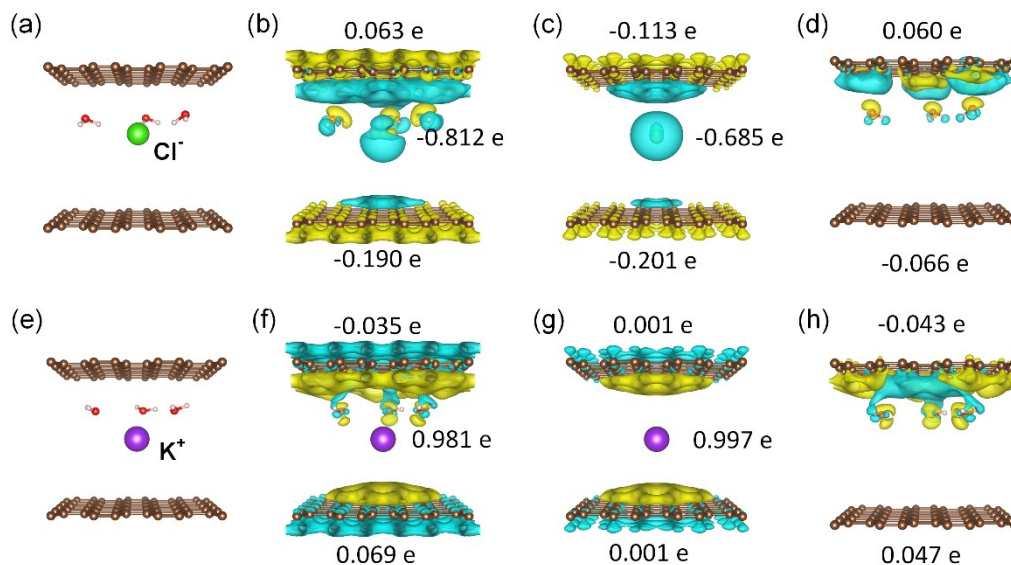
As shown in Table S1, the interactions among ions, graphene and water molecules were described by the empirical force field, which indicates that the polarization of graphene was not considered particularly. It was estimated from experiments that the surface charge density of graphite walls is smaller than  $20 \mu\text{C m}^{-2}$ , which is equivalent to only one unit charge per  $8011 \text{ nm}^2$ .<sup>S6</sup> We think this tiny surface charge density directly prove that the polarization effect might be not significant for ion transport through graphene channels. The comprehensive competition among graphene-ions interactions, ion-water interactions, graphene-water interactions and water-water interactions needs to be taken into account. Our previous work supports that graphene-water interactions and water-water interactions are dominant factors.<sup>S7</sup> To this end, here we carried out quantum calculations of hydrated ions (Cl<sup>-</sup> and K<sup>+</sup>) between two graphene layers with a spacing of  $10.2 \text{ \AA}$ , as shown in Figure S1 (a/e). The electronic calculations were performed based on the density functional theory (DFT) as implemented in the Quantum Espresso package.<sup>S8</sup> The exchange and correlation interaction between electrons are treated by the Perdew-Burke-Ernzerhof (PBE) functional,<sup>S9</sup> and the projector-augmented wave (PAW) method<sup>S10</sup> with a plane wave kinetic energy cutoff of 60 Ry. A Monkhorst-Pack grid of size of  $6 \times 6 \times 1$  was used to sample the surface Brillouin zone. The charge transfer between the hydrated ions and graphene was characterized by the Bader charge analysis algorithm.<sup>S11</sup> The differential charge density is defined as:

$$\Delta\rho(\mathbf{r})=\rho_{\text{tot}}(\mathbf{r})-\rho_{\text{Hyd-ion}}(\mathbf{r})-\rho_{\text{GRA}}(\mathbf{r}), \quad (\text{A1})$$

in which  $\rho_{\text{tot}}$  is the total electron density of the whole system,  $\rho_{\text{Hyd-ion}}$  and  $\rho_{\text{GRA}}$  denote the electron densities for hydrated ions and graphene sheets, respectively.

The differential charge density was plotted in Figure S1 (b/f), respectively. We also compared the differential charge density with the systems containing only “graphene + ions (Figure S1 (c/g))” or “graphene + water molecules (Figure S1 (d/h))”. According to their distribution profiles, Cl<sup>-</sup> and K<sup>+</sup> ions were placed at the positions  $4.14 \text{ \AA}$  and  $5.1 \text{ \AA}$  away from one graphene sheet, respectively.<sup>S7</sup> We can find that the major

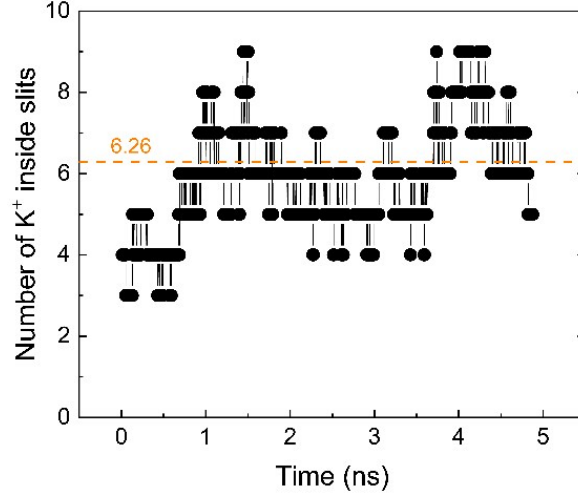
contribution to the polarization of graphene comes from the graphene-water interactions, rather than graphene-ion interactions. We believe that the interfacial polarization between graphene and water has been taken into account in the force field parameters.<sup>S2</sup> For these reasons, we conservatively employed the empirical force field from literatures.



**Figure S1.** Quantum calculations on charge transfer between graphene and ions/water. (a/e) Simulation model for hydrated  $\text{Cl}^-$  ( $\text{K}^+$ ) between two graphene layers with a spacing of  $10.2 \text{ \AA}$ , which is corresponding to  $h = 6.8 \text{ \AA}$ . The models here only contain three water molecules for simplicity and to speed up the calculations. (b/f) Isosurfaces of differential charge density for the two systems shown in (a/e). (yellow: accumulation; cyan: depletion) isovalue =  $0.002 \text{ e/Bohr}^3$ . (c/g) Isosurfaces of differential charge density for bare ions confined between two graphene sheets. (d/h) Isosurfaces of differential charge density for only three water molecules confined between two graphene sheets.

### III. Ion concentration inside 2D slits.

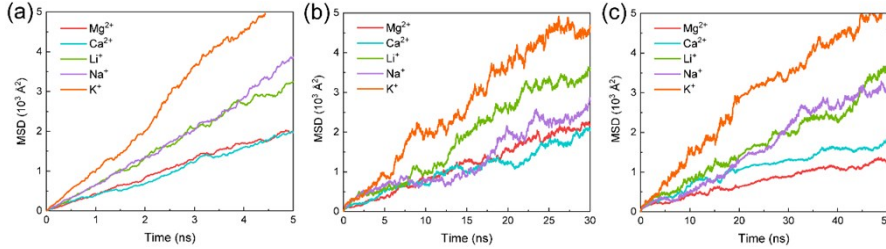
As been discussed in the main text, from  $I = \mu cvEFS$ , we can anticipate that the ion mobility is one of the most important variables to determine  $I$ , under the precondition since  $cv$  is a constant for all the chloride solutions in the present work. To check this, we performed MD simulations to calculate the ion concentration inside the slits. As shown in the Figure S2, the results exhibit considerable fluctuations. Given the limitation on our simulation systems,  $1 \text{ mol/L}$  corresponds to  $6.26$  monovalent cation inside the slit. Within a simulation of  $5 \text{ ns}$ , our results give a range between  $3$  and  $9$ . The value of  $6$  with the maximum probability proves that the ion concentration inside the slit is generally equal to that in the reservoir in this case. This is understandable since the energy barrier of  $\text{K}^+$  ions entering into a  $h = 6.8 \text{ \AA}$  2D slit is not very large compared with the typical kinetic energy. For larger energy barriers, for example, bivalent ions and  $h = 3.4 \text{ \AA}$  slit, one need to be more cautious and more MD simulations with even larger system are required to reduce fluctuations of the results.



**Figure S2.** Number of  $K^+$  ions inside 2D slits ( $h = 6.8 \text{ \AA}$ ). The ion concentration outside is 1 mol/L, which corresponds the number of ions inside is 6.26 (Horizontal dash line).

#### IV. Ion mobilities calculated using the Einstein relation

We calculated the ion mobilities using the Einstein relation,<sup>S12</sup>  $\mu = Dq/k_B T$ , in which  $q$  is the ionic charge,  $k_B$  is the Boltzmann constant, and  $D$  is the ionic diffusion coefficient.  $D$  is proportional to the slope of mean-squared displacement (MSD) versus time,  $k$ , as shown in Figure S1. MSD and ion mobilities were calculated in three scenarios, (i) bulk solution; (ii) only inside 2D slits without the entry effect; (iii) two reservoirs connected by 2D slits with the entry effect incorporated.



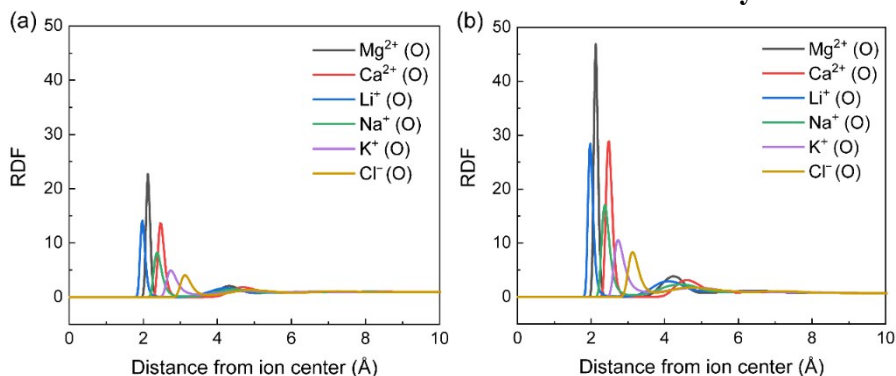
**Figure S3.** Mean-squared displacement calculated from MD simulations for various cations in three scenarios. (a) bulk solution; (b) only inside 2D slits without the entry effect; (c) two reservoirs connected by 2D slits with the entry effect incorporated.

Table S2. Slope of MSD and ion mobilities

Ion type	Bulk solution		Only inside 2D slits		2D slits with entry effect	
	$k$	mobility	$k$	mobility	$k$	mobility
$Mg^{2+}$	4.193	5.443	0.662	2.578	0.204	0.793
	( $\pm 0.002$ )	( $\pm 0.08$ )	( $\pm 0.003$ )	( $\pm 0.12$ )	( $\pm 0.002$ )	( $\pm 0.08$ )
$Ca^{2+}$	3.948	5.125	0.759	2.956	0.210	0.819
	( $\pm 0.002$ )	( $\pm 0.08$ )	( $\pm 0.004$ )	( $\pm 0.18$ )	( $\pm 0.002$ )	( $\pm 0.08$ )
$Li^+$	6.661	4.323	1.401	2.728	0.655	1.276
	( $\pm 0.003$ )	( $\pm 0.06$ )	( $\pm 0.013$ )	( $\pm 0.26$ )	( $\pm 0.008$ )	( $\pm 0.15$ )
$Na^+$	7.183	4.662	0.880	1.713	0.649	1.264
	( $\pm 0.002$ )	( $\pm 0.05$ )	( $\pm 0.011$ )	( $\pm 0.22$ )	( $\pm 0.009$ )	( $\pm 0.19$ )
$K^+$	11.340	7.360	1.694	3.298	0.766	1.492
	( $\pm 0.003$ )	( $\pm 0.06$ )	( $\pm 0.013$ )	( $\pm 0.26$ )	( $\pm 0.012$ )	( $\pm 0.23$ )

Units:  $k$ :  $10^{-5} \text{ cm}^2/\text{s}$ ; mobility:  $10^{-4} \text{ cm}^2/(\text{V s})$

## V. Radial distribution function and coordination number of hydrated ions



**Figure S4.** The radial distribution function of water molecules around each ion in (a) bulk aqueous and (b) graphene slits with a height of 6.8 Å.

**Table S3.** Ion hydration radius and coordination number (CN). The ion hydration radius,  $r$ , of the first and second hydration shells (HSs) were obtained as the first and the second minimum from the RDF curves.

	Bulk				$h = 6.8 \text{ \AA}$ slits			
	1 <sup>st</sup> HS		2 <sup>nd</sup> HS		1 <sup>st</sup> HS		2 <sup>nd</sup> HS	
	$r$ (Å)	CN	$r$ (Å)	CN	$r$ (Å)	CN	$r$ (Å)	CN
Mg <sup>2+</sup>	2.65	5.97	5.08	20.05	2.7	6.0	5.07	17.95
Ca <sup>2+</sup>	3.32	7.96	5.67	27.29	3.42	7.94	5.98	24.02
Li <sup>+</sup>	2.68	4.16	5.1	19.46	2.72	4.16	5.56	19.25
Na <sup>+</sup>	3.16	5.73	5.46	23.28	3.16	5.88	5.53	19.94
K <sup>+</sup>	3.64	7.06	5.75	26.55	3.59	7.12	5.89	21.95

## References

- S1 H. Berendsen, J. Grigera and T. Straatsma, The missing term in effective pair potentials, *J. Phys. Chem.*, 1987, **91**, 6269–6271.
- S2 Y. Wu and N. Aluru, Graphitic carbon–water nonbonded interaction parameters, *J. Phys. Chem. B*, 2013, **117**, 8802–8813.
- S3 G. Chen, Y. Guo, N. Karasawa and W. A. Goddard III, Electron-phonon interactions and superconductivity in K<sub>3</sub>C<sub>60</sub>, *Phys. Rev. B: Condens. Matter*, 1993, **48**, 13959.
- S4 P. Li and M. K. Merz Jr, Taking into account the ion-induced dipole interaction in the nonbonded model of ions, *J. Chem. Theory Comput.*, 2014, **10**, 289–297.
- S5 I. S. Joung and T. E. Cheatham, Determination of alkali and halide monovalent ion parameters for use in explicitly solvated biomolecular simulations, *J. Phys. Chem. B*, 2008, **112**, 9020–9041.
- S6 A. Esfandiar, B. Radha, F. Wang, Q. Yang, S. Hu, S. Garaj, R. Nair, A. Geim and K. Gopinadhan, Size effect in ion transport through angstrom-scale slits, *Science*, 2017, **358**, 511–513.
- S7 Y. Z. Yu, J. C. Fan, A. Esfandiar, Y. B. Zhu, H. A. Wu and F. C. Wang, Charge asymmetry effect in ion transport through angstrom-scale channels, *J. Phys. Chem. C*, 2019, **123**, 1462–1469.
- S8 P. Giannozzi, S. Baroni, N. Bonini, M. Calandra, R. Car, C. Cavazzoni, D. Ceresoli, G. L. Chiarotti, M. Cococcioni, I. Dabo, A. Dal Corso, S. de Gironcoli, S. Fabris, G. Fratesi, R. Gebauer, U. Gerstmann, C. Gougoussis, A. Kokalj, M. Lazzeri, L. Martin-Samos, N. Marzari, F. Mauri, R. Mazzarello, S. Paolini, A. Pasquarello, L. Paulatto, C. Sbraccia, S. Scandolo, G. Sclauzero, A. P.

- Seitsonen, A. Smogunov, P. Umari and R. M. Wentzcovitch, QUANTUM ESPRESSO: a modular and open-source software project for quantum simulations of materials, *J. Phys. Condens. Matter*, 2009, **21**, 395502.
- S9 J. P. Perdew, K. Burke and M. Ernzerhof, Generalized gradient approximation made simple, *Phys. Rev. Lett.*, 1996, **77**, 3865–3868.
- S10 P. E. Blöchl, Projector augmented-wave method, *Phys. Rev. B*, 1994, **50**, 17953–17979.
- S11 W. Tang, E. Sanville and G. Henkelman, A grid-based Bader analysis algorithm without lattice bias. *J. Phys. Condens. Matter*, 2009, **21**, 084204.
- S12 S. Koneshan, C. Rasaiah, R. Lynden-Bell and S. Lee, Solvent structure, dynamics, and ion mobility in aqueous solutions at 25 °C, *J. Phys. Chem. B*, 1998, **102**, 4193–4204.